Journal of Structural Geology, Vol. 3, No. 3, pp. 219 to 229, 1981.
Printed in Great Britain

0191-8141/81/030219-11 $02.00/0
Pergamon Press Ltd.

Strain patterns of pluton emplacement in a crust undergoing non-coaxial deformation, Sierra Morena, Southern Spain*

J. P. BRUN

Laboratoire de Géologie Structurale, Centre Armoricain d'Etude Structurale des Socles, Avenue du General Leclerc, 35042 Rennes Cédex, France

and

J. PONS

Laboratoire de Géologie-Pétrologie, Université Paul Sabatier, 38 Rue des trente-six ponts, 31078 Toulouse Cédex, France

(*Received* 24 *October* 1980; *accepted in revised form* 11 *May* 1981)

Abstract—This paper investigates the problem of interference between regional and local strain fields, the latter corresponding to a pluton ballooning. Natural examples from the Sierra Morena (Southern Spain) are described. Two distinct patterns have been recognised, according to whether transcurrent motions or thrusting motions predominate in the regional deformation.The map of foliation trajectories shows typical features such as triple points and geometric continuity between pluton internal fabric and country rock cleavage even when these are oblique to the contact.

A simple mathematical model of interference between ballooning and simple shear is presented. In this model, the ballooning may be circular or elliptical. The model is used to predict the position of triple points, patterns of principal trajectories and variations of finite strain. A comparison is made with plutons from the Sierra Morena.

INTRODUCTION

AROUND many granitic plutons, an intense deformation of country rocks can be observed. This spectacular effect, which was previously called 'pushing aside' or 'forceful intrusion' is a consequence of the diapiric nature of granitoid body emplacement. It is well known that plutons rise in the continental crust rather like elongated bubbles or 'mongolfieres' (Grout 1945, Ramberg 1967, 1970, Fyfe 1973). Because plutonic rocks are lighter than many sedimentary rocks, the pluton ascent can be attributed to the buoyancy forces resulting from this difference of density. When the buoyancy forces decrease, or when the viscosity increases as a result of cooling during ascent, or when an obstacle presents itself on the way up, the top of a pluton will come to a halt whilst the tail-end will continue to rise, inflating or 'ballooning' the pluton. An alternative mechanism that can explain the ballooning is the continuous flow of magma into the mongolfiere along a vertical pipe from a magma chamber beneath (see Whitehead & Luther 1975). But because this mechanism needs a very low magma viscosity, it probably does not apply to actual granitoid magma that is emplaced as crystalline mush (Berger & Pitcher 1971, Pitcher 1979). The kinematic model of ballooning devised by Ramsay (1981), allows us to calculate the pluton diameter increase from finite strain measurements (Ramsay 1981, Holder 1979, 1981). Little attention has been paid to the consequences of ballooning in the country rocks (Clifford 1972, Schwerdtner 1972, Morgan 1980). Such studies should be very useful in those orogenic belts where granitoid plutons are numerous. In orogenic belts, some plutons are emplaced during regional deformation events, intrusive effects then interfere with regional deformation effects (Ledru & Brun 1977, Brun & Pons 1979, 1981). In this paper, the example of Sierra Morena granitoids is described. A model of interference between a regional strain field and local ballooning fields is put forward, using maps of principal strain directions. Two patterns are distinguished according to the orientations of shearing planes in the regional deformation, (horizontal or vertical). A simple mathematical model of interference between ballooning and simple shear is presented and the results are compared with the example of the Sierra Morena plutons.

INTERFERENCE BETWEEN REGIONAL SHEAR AND PLUTON BALLOONING IN THE BURGUILLOS ANTICLINE (SOUTHERN SPAIN)

The plutons

Our intention is not to enter in great detail into the petrology and the structure of the plutons, these will be

* Presented at a conference on Diapirism and Gravity Tectonics organised by the Tectonic Studies Group at the University of Leeds, 25–26 March 1980.

dealt with at greater length in a future publication.

In the Hercynian segment of the S.W. Iberian Peninsula (Sierra Morena Occidental) metamorphic belts alternate with zones where numerous Hercynian batholiths are well exposed. The latter were essentially emplaced in elongate NW–SW anticlinal structures overturned towards the SW (Bard 1969).

The plutons studied in the present work occur in the Burguillos–Monesterio Anticlinorium (Fig. 1): the intrusions of Burguillos del Cerro, Valencia del Ventoso, Salvatierra and most of the Brovales intrusion were emplaced in a Precambrian psammitic–pelitic sequence forming the axial zone of this large structure; only the southern termination of the Brovales massif cross-cuts the Cambrian calcareous sediments forming the SW limb.

These massifs are roughly ovoid or elliptic. The Salvatiera intrusion is elongated parallel to the anticlinical axis, whereas the Burguillos, Valencia and Brovales complexes are elongated more or less perpendicular to this direction. Furthermore, they present a zonal arrangement of rock types characterized by an off-centred core (more basic) lying towards the NE. The internal structures, compositional layering in gabbroic varieties and alignment of planar elements due to fluid flow in other types, are also arranged concentrically and eccentrically. All these features indicate dome-shaped geometries expanded in the SW or SSW direction, i.e. in the direction in which the anticlines are overturned. Besides, all the linear fluid structures of these massifs are oriented in this direction. In contrast, the Salvatierra massif is almost parallel to the anticlinal axis and has a typical helicoidal internal structure.

The various compositions of these plutons (essentially gabbroic for the Burguillos complex, intermediate for the Valancia and Brovales complexes, and granitic for the Salvatierra massif) seem to illustrate the increasingly differentiated products of a single calc-alkaline trend. The order of emplacement may correspond to the order of differentiation. Geochronological data (Dupont *et al.* in press) confirm this assumption and, furthermore, indicate that the period of emplacement was contemporary with the Hercynian tectonic phases (Table 1).

Tectonic setting of the Burguillos anticline

The Burguillos–Monestiero anticline, in which the plutons are situated, is located between two major tectonic units of the South Iberian Hercynian belt: the Badajoz–Cordoba shear zone and the Fregenal de la Sierra nappes (Fig. 1). The Burguillos anticline, overturned toward the SW, is probably the root zone of the Fregenal nappes. In the nappes, two phases of defor-

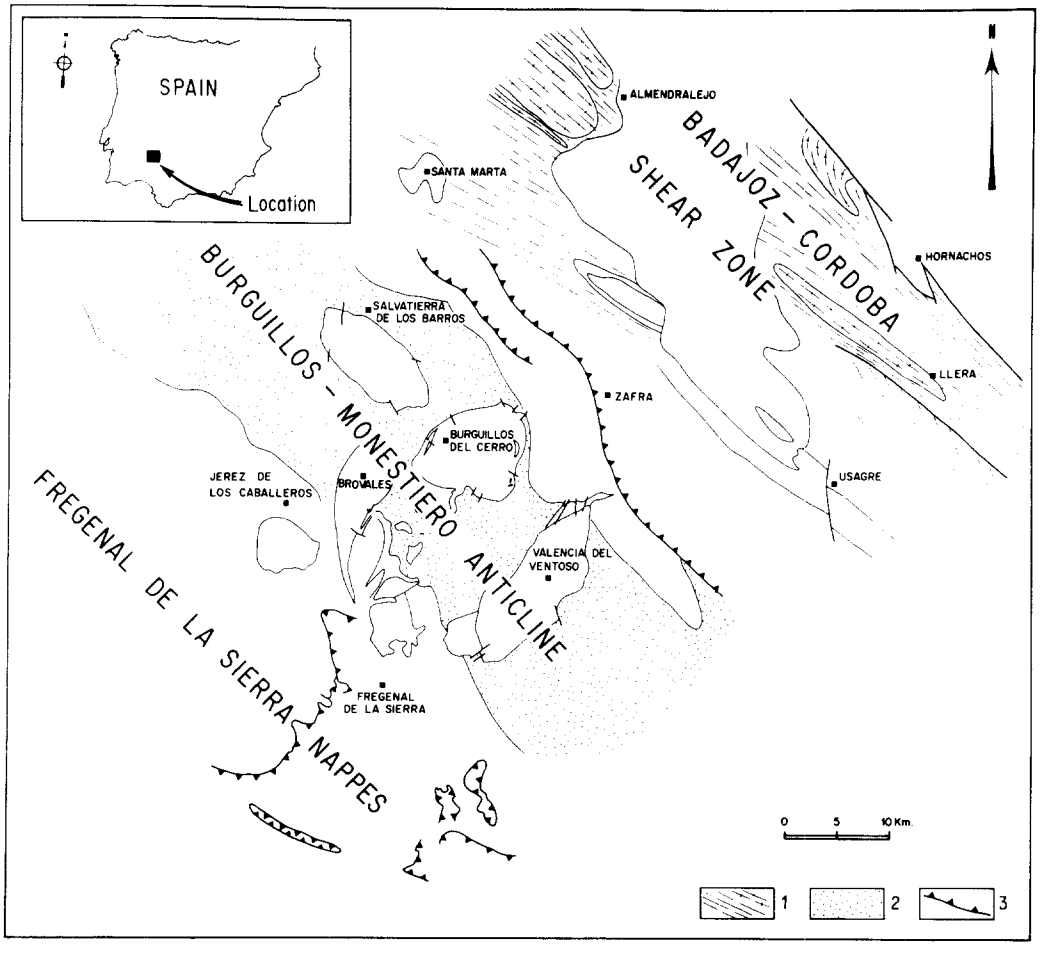

Fig. 1. Structural setting of the Burguillos anticline intrusions. (1) Foliation trends in the Badajoz–Cordoba shear zone, (2) Precambrian sediments in the Burguillos anticline, (3) Thrust faults.

Table 1. Time relations between deformation events and pluton emplacement in the studied area

Deformation events	Structure	Kinematics	Pluton emplacement
1	Burguillos anticline	Thrusting toward the SW	Burguillos (1) Valencia (2) Brovales (3)
2		Sinistral transcurrent shear parallel to the anticline axis	Salvatierra (4)

mation have been distinguished (Vauchez 1975). The first phase, corresponding to nappe emplacement, produced recumbent folds and a flat axial plane foliation. The main features of the second phase are a subvertical foliation, trending NW–SE, and upright folds which produce type 3 interference patterns (Ramsay 1962) on the map scale (Vauchez 1975), where they intersect first-phase folds.

The Badajoz–Cordoba shear zone is a sinistral shear zone, several kilometres wide, developed in Precambrian sediments and Hercynian granites (Bladier & Laurent 1974, Burg *et al.* 1980). Between Santa Marta and Almendralejo the foliation in blastomylonites is gently dipping over several kilometres (Fig. 2) and becomes progressively vertical toward the NE boundary of the zone. The strong stretching lineation, mainly subparallel to the strike of the zone is compatible with a transcurrent shear zone, however, the flat-lying associated foliation could indicate a thrusting component of the NE block over the SW block. Between Usagre and Llera, zones of vertical foliation alternate with zones of flat foliation frequently folded by folds with axes parallel to the stretching lineation. This indicates that the flat foliation developed early and that the inferred thrusting component, if any, acted early in the deformation history. Moreover lateral variations, from one cross section to another, and temporal variations, forming a transition from a simple thrusting to mixed thrusting and transcurrent shear, show the complexity of the deformation history in this shear zone.

In the Burguillos anticline, the Cambrian basal units and the Proterozoic sediments are affected by a heterogeneous penetrative deformation. Heterogeneities can be detected in principal strain orientations or in strain intensity. Mapping of foliation and stretching lineation helps to demonstrate that strain heterogeneities are spatially related to pluton shapes.

Foliation trajectories

Systematic measurements of the foliation in the sediments were made. Where strain markers (sedimentary clasts, pellets, fossils, metamorphic spots) were present, it was evident that the foliation was developed parallel to the principal flattening plane. In the plutonic rocks, the planar mineral fabric was measured. Although this plane is poorly developed, and difficult to measure on the outcrop, it was also verified that the foliation corresponds to the flattening plane of inclusions. This relationship has been confirmed by petrofabric analysis (Pons 1975). Because of their significance in terms of flattening, the foliation in sediments and the planar fabric in plutonic rocks are shown on the maps (Fig. 3) with the same symbol. Several interesting points arise from examination of the maps. Outside the zone of plutons, the foliation direction is NW–SE and parallel to the axis of the anticline (Fig. 3). Perturbation of this trend can be seen between and at the contacts of the plutons. Around the plutons the foliation tends to become parallel to the pluton boundaries. The transition between the regional trend and the trend of the foliation around the plutons is progressive, and locally characterized by triple points (Fig. 3). At these triple points the ellipsoid of finite strain approaches a prolate spheroid (see discussion of model). These triple points are more or less clearly defined depending on the density of the data. The map of foliation dip (Fig. 4) shows that the area located between the Brovales, Burguillos and Valencia plutons has gentle to intermediate dips. Areas at the NW or SE ends of this group of plutons have a subvertical foliation.

Stretching lineation

In the Proterozoic sediments, the stretching lineation is

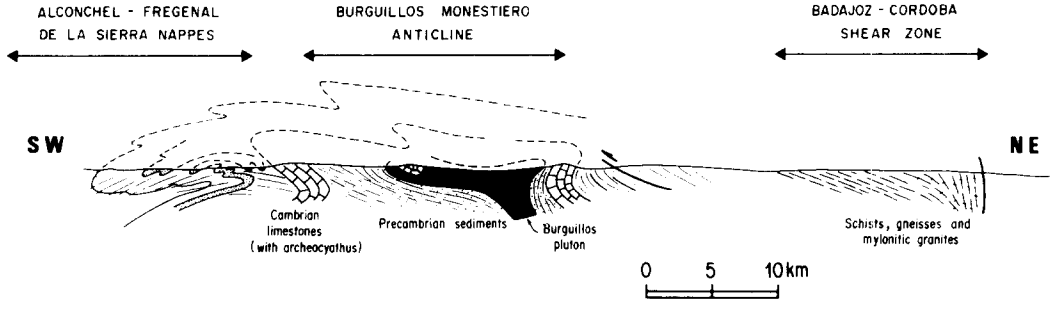

Fig. 2. Schematic cross section showing structural relations between the main tectonic units of the studied area.

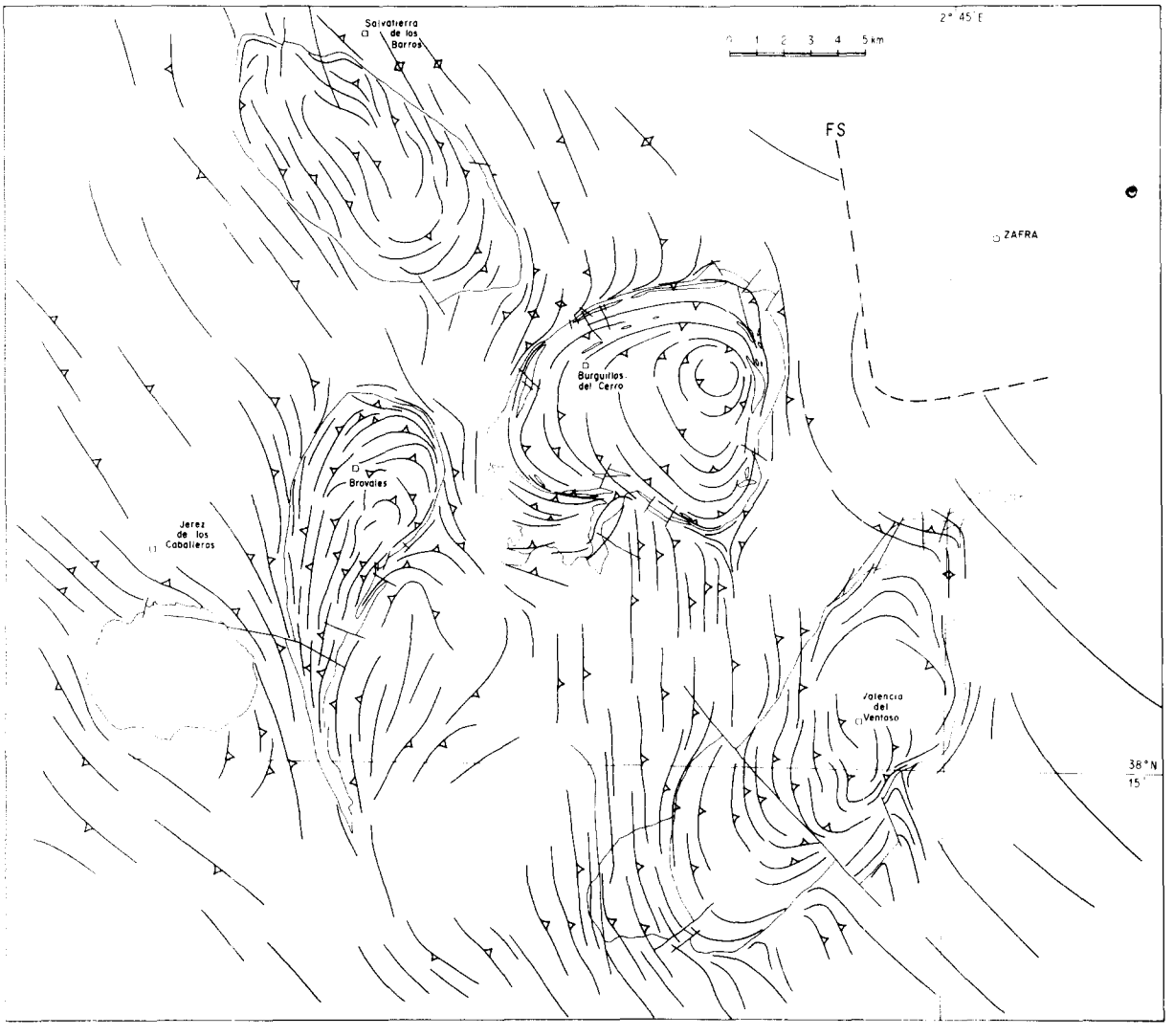

Fig. 3. Foliation trajectories in the Burguillos anticline. FS is foliation front.

indicated by the stretching of quartz grains and metamorphic spots (cordierite, andalusite) or by the alignment of minerals. Field observations show that stretching is more intense in the area between the Brovales, Burguillos and Valencia plutons. The map of lineation trajectories (Fig. 5) shows, for this area, a NE–SW orientation that contrasts with the NW–SE orientation outside it.

Superimposed small-scale structures

Superimposed small scale structures have been observed in the area between the Brovales, Burguillos and Valencia plutons, which show an anomaly in foliation and lineation orientations.

Foliations and lineations are locally folded. Folds are asymmetric, have axes parallel or slightly oblique to the stretching lineation, and show a constant NW vergence. In most of the observed cases, folds were apparantly related to initial heterogeneities such as dykes of eruptive material or quartz veins, and were associated with a crenulation cleavage. Similar observations have been made in the area located on the SW side of the Brovales pluton 'tail' (Fig. 3) and around the Jerez pluton where the foliation is also gently dipping.

Progressive deformation in the Burguillos anticline

Deformation in the Burguillos anticline was previously ascribed to two superimposed deformation phases and the pluton was regarded as having been emplaced after the second phase (Bard 1965, 1969). The data given above show that pluton emplacement was synkinematic and that the deformation history was progressive rather than polyphase.

The criteria that may be used to demonstrate that the plutons were emplaced synkinematically are mainly: (a) stretching of thermal spots, (b) geometrical continuity between deformation features (foliation and lineation) as one passes from plutonic rocks to country rocks across the thermal aueroles and (c) the configuration of the finite strain trajectories. The third criterion has been discussed previously by Ledru & Brun (1977). According to these authors the development of triple points requires that the ballooning and regional deformation must be at least partly synchronous. If plutons are emplaced after regional deformation then the deformation resulting from ballooning in the country rocks will be superimposed on previously developed structures and a previous foliation at

the external boundary of distended country rocks will be refolded or crenulated. The local obliquity between the foliation trajectories and the contact of the plutons which is due to a negligible viscosity contrast between plutonic rocks and country rocks, shows also that "plutons are syntectonic in the strictest sense" (Berger & Pitcher 1970, p. 452). Taking into account the features shown on foliation and lineation maps and the local existence of superposed small-scale structures and petrological data, we are able to propose the following progressive deformation scheme.

The regional deformation started with a tangential shear component toward the SW giving rise to an overturned anticline. The Burguillos and Valencia plutons and probably also the Brovales pluton were emplaced during this event. The thermal softening of country rocks consequent to pluton emplacement favours deformation, and consequently the development of a flat to intermediate NE dipping foliation, and of a NE plunging stretching lineation. The plutons are elongated in the lineation direction, the more so as their ascent was evidently slackened, if not stopped, by the Cambrian limestones. This deformation episode can be related to the sense of thrusting observed in the Badajoz–Cordoba shear zone, and to the emplacement of the Fregenal nappes.

This first episode was followed by a sinistral transcurrent shear movement subparallel to the anticline axis. The resulting foliation is vertical and oriented NW–SE. The stretching lineation plunges alternatively toward the NW and the SE. The Salvatierra pluton was emplaced during this second episode and is elongated along the anticline axis. Its helicoidal internal foliation attests to the sinistral shear. In the area of flat foliation asymmetrical fold, compatible with a sinistral shear component, developed. The Brovales pluton is strongly deformed by a shear zone

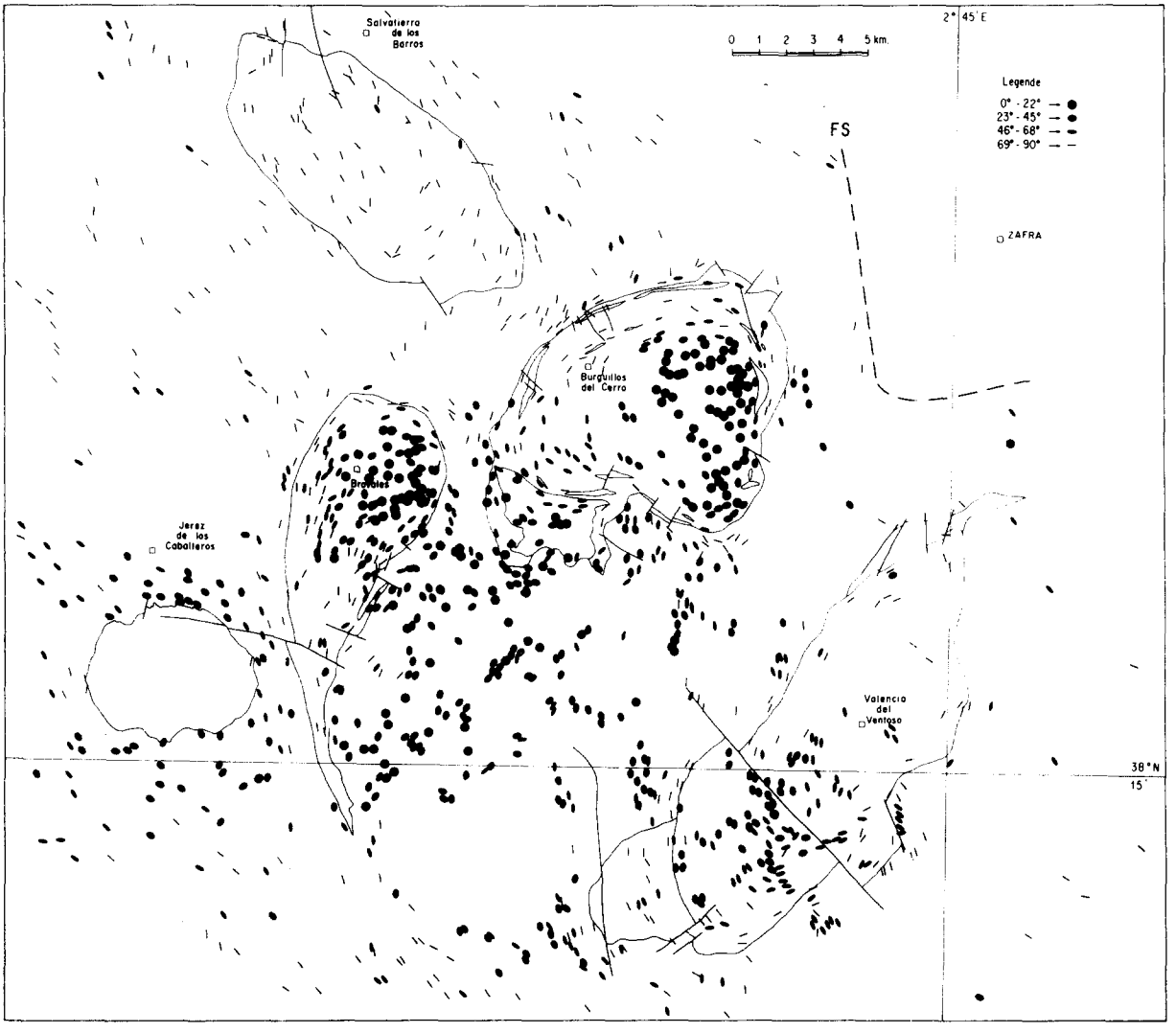

Fig. 4. Dip variations of foliation in the Burguillos anticline. Small circles and lines are respectively horizontal and vertical dips. Two classes of intermediate dips are presented by elipses. Zones of flat-lying foliation appear dark while zones of straight dipping foliation appear clear.

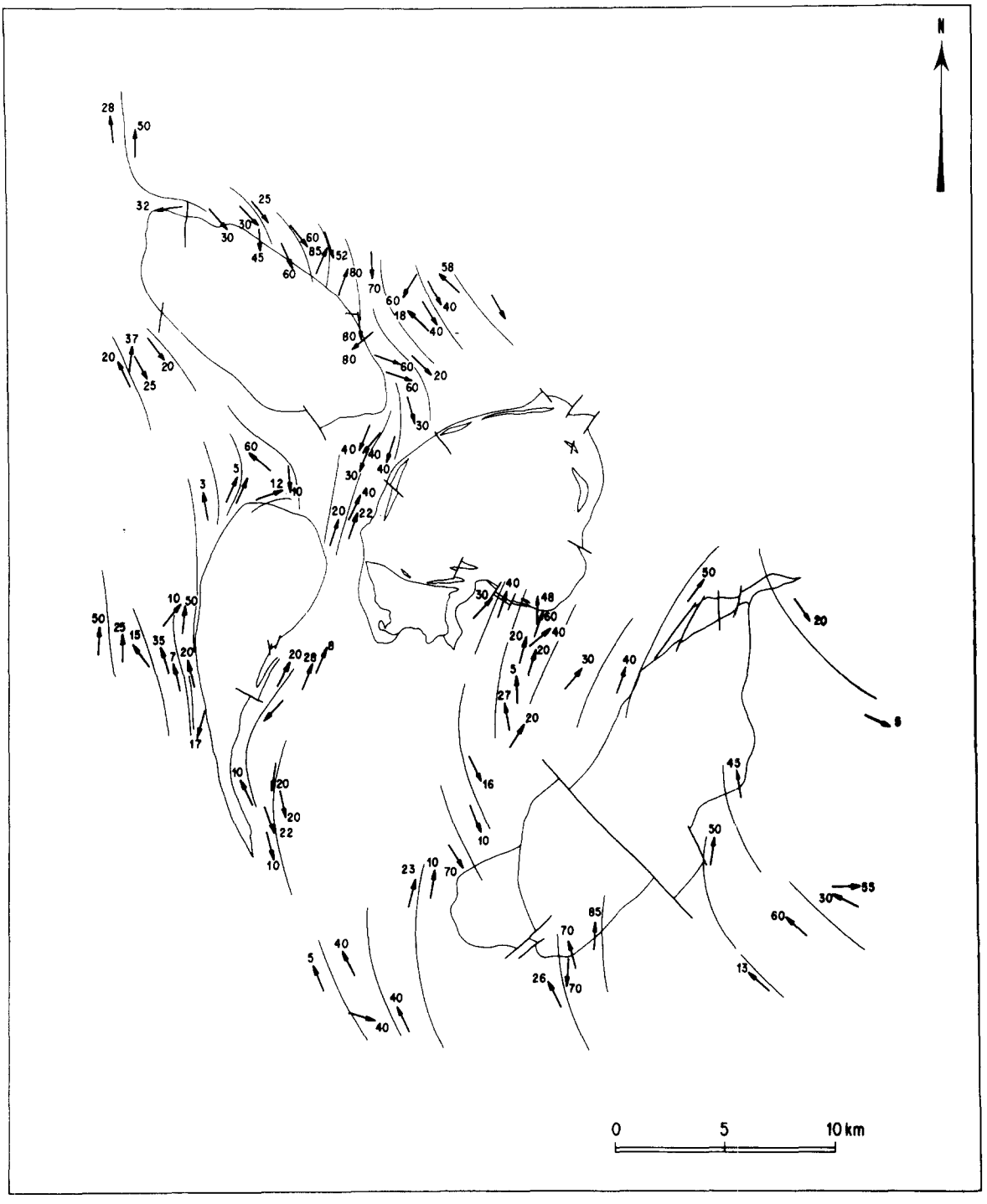

Fig. 5. Stretching lineation map. Solid lines indicate mean trends of lineation.

on its SW boundary, giving rise to the classical shape of an asymmetrical drop (Berthé *et al.* 1979). This second episode can be related to the purely transcurrent behaviour of the Badajoz–Cordoba shear zone and probably to the second phase of deformation in the Fregenal nappe area.

No clear boundary has been found between low dip and vertical foliation domains. The transition is, on the contrary, continuous. Therefore the deformation in the Burguillos anticline can be interpreted as progressive, giving rise locally to superposed structures.

The two interference patterns

The finite strain features associated with pluton emplacement can be summarised in two distinct patterns (Fig. 6). Pattern A, which is seen in the Burguillos and Valencia plutons, is due to an interference between ballooning and thrusting shear. Pattern B, which is seen in Salvatierra pluton, is due to interference between a ballooning and a transcurrent shear. These two patterns have in common the existence of foliation triple points and local obliquities of foliation at the boundaries of the

	PATTERN A Type : Burguillos - Valencia	PATTERN B Type : Salvatierra
Triple point (◄) Trace and dip of flattening plane Stretching lineation	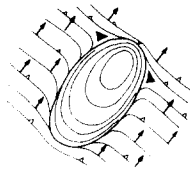	
PLUTON ORIENTATION	Sub-orthogonal to the anticline axis	Sub-parallel to the anticline axis
FOLIATION DIP IN COUNTRY ROCKS	Flat or intermediate	Vertical
FOLIATION TRAJECTORIES IN PLUTONS	Eccentric	Helicoidal
STRETCHING LINEATION	Sub-orthogonal to foliation strike	Sub-parallel to foliation strike
SHEAR COMPONENT	THRUSTING SHEAR	TRANSCURRENT SHEAR

Fig. 6. The two types of finite strain patterns resulting from interference between ballooning and regional shear in the Burguillos anticline. Open triangles indicate dip of foliation and arrows show the plunge of lineations.

plutons. On the other hand, they differ in the relative pluton–anticline orientation, in the foliation dip and foliation pattern in the plutons (Fig. 6). The Brovales pluton may be compared with Pattern A in its NE part.

A SIMPLE MATHEMATICAL MODEL OF INTERFERENCE BETWEEN BALLOONING AND SIMPLE SHEAR

The simple mathematical model presented in this second part of the paper is a test of the interpretation proposed earlier. In this model, displacements corresponding to a simple shear are combined with those corresponding to pluton ballooning. Resulting displacements are used to compute finite strain. Maps of finite strain variations around a pluton in a medium undergoing simple shear are produced that can be compared with natural examples. Only the case of 'transcurrent simple shear' has been developed (Fig. 6, pattern B) but the results can be adapted easily to the case of 'thrusting simple shear' (Fig. 6, pattern A).

Pluton ballooning

In the Burguillos anticline, most of the granitoid plutons are emplaced in the Proterozoic sediments and have not pierced the Cambrian limestones. It is likely that Cambrian strata provided an obstacle to the ascent of the plutons and that the plutons were inflated under the Proterozoic–Cambrian interface (Fig. 7).

When a pluton inflates, the country rocks are radially displaced outward. To simulate such displacements we have chosen a law:

$$U_r = \frac{G}{r}, \tag{1}$$

where U_r is the radial displacement of a point initially situated at a distance r from the centre of the pluton and G is the 'ballooning parameter'. Equation (1) has been inspired by equations (20 and 21, p. 239) derived by Jaeger & Cook (1969) for displacements around a cylindrical hole in a stressed elastic medium. In the future, more realistic inflation laws should be deduced from strain measurements in natural inflated plutons (Holder 1979, Ramsay 1981).

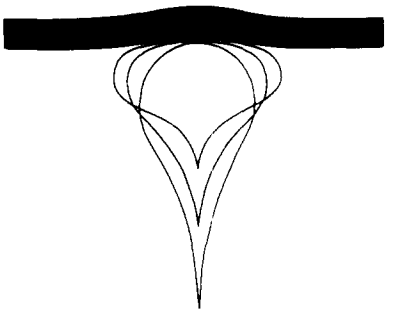

Fig. 7. A possible model for pluton ballooning in the Burguillos anticline. The mongolfiere is stopped by a competent layer and then settles on itself increasing its diameter.

To simplify the computation, in the following model, the displacements are considered in the final maximum diameter plane of the pluton. It follows that this plane is a symmetry plane of the finite strain.

Displacement equations

The pluton is situated at the centre of a square grid, of 25 × 25 points. Each point (X, Y) is displaced radially (1) and laterally, parallel to the X axis (Fig. 8). Relations between initial (X, Y) and final (X', Y') coordinates of the point, after a displacement due only to ballooning are after (1)

$$X' = \left(\frac{r^2+G}{r}\right)\cos\alpha, \tag{2a}$$

$$Y' = \left(\frac{r^2+G}{r}\right)\sin\alpha \tag{2b}$$

α, being the angle between the radius and the X coordinate axis. The displacements corresponding to the simple shear are:

$$Ux = \gamma Y', \tag{3a}$$

$$Uy = 0 \tag{3b}$$

where $\gamma = \tan\psi$, ψ being the angular shear strain along X (Fig. 8).

In combining (2) and (3), we obtain the final coordinates:

$$X'' = \left(\frac{r^2+G}{r}\right)(\cos\alpha + \gamma\sin\alpha) \tag{4a}$$

$$Y'' = \left(\frac{r^2+G}{r}\right)(\sin\alpha). \tag{4b}$$

In a first type of model, for given values of G and γ, the final positions of the 625 points of the grid are computed using (4a) and (4b). With the initial (X, X) and final $(X'',$

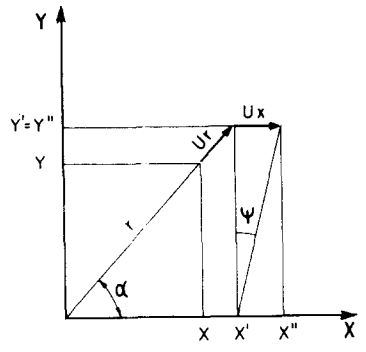

Fig. 8. Displacement of points in a model of interference resulting successively from a ballooning (Ur) and a simple shear (Ux). See explanation in the text.

Y'') coordinates of a given point one can compute the finite strain state at this point (cf. Appendix).

In a second type of model, the ballooning is elliptical. The pluton has initially a slightly elliptical section whose principal axes are respectively A along Y and B along X. Inflating in a given direction is proportional to the initial radius in this direction. The ballooning parameter G must be replaced in (4a) and (4b) by Ge:

$$Ge = G(\sin^2\alpha + (B^2/A^2)\cos^2\alpha)^{1/2}. \quad (5)$$

Pluton shape

When the ballooning is circular combined with a shear component, the final shape of the pluton is elliptical. The axial ratio of the pluton section corresponds to the axial ratio of the strain ellipse for simple shear (Fig. 9). When the ballooning is elliptical, the final shape of the pluton may be complex, nearly elliptical if the A/B ratio is close to 1 (Fig. 10a), in the shape of a constricted ellipse if the A/B ratio decreases (Fig. 10b).

Flattening plate trajectories and triple points

For each point (with X'', Y'' coordinates) the orientation of the principal flattening plane has been calculated (Figs. 9 and 10). The trace of the flattening plane is closed in the pluton area but quickly becomes rectilinear at a certain distance from this area (Figs. 9 and 10) at the extremities of the pluton elliptical section, we note the existence of triple points. According to the value of the R/G ratio (pluton initial radius over ballooning parameter), the triple points are internal or external to the pluton (Fig. 9). The internal position corresponds to a low value of ballooning. When the ballooning is elliptical, the position of the triple points is slightly asymmetrical with respect to the pluton shape (Fig. 10). In this case, the trajectories of the flattening plane show a regular sense of obliquity at the pluton boundaries (Fig. 10).

Variations of the finite strain ellipsoids

The strain ellipsoid shape can be represented by a parameter such as K (Flinn 1962) ($K = (\lambda_1/\lambda_2 - 1)/(\lambda_2/\lambda_3 - 1)$, with $\lambda_1 > \lambda_2 > \lambda_3$). A map of K values shows that the finite strain in the pluton area of flattening type ($K < 0.7$, Figs. 11a & b and Fig. 12a). Outside this area, the finite strain is close to plane strain ($1.0 > K > 0.7$). A comparison of K-value maps for circular (Fig. 11a) and elliptical (Fig. 12a) ballooning shows that finite strain variations are only slightly different in the two types of model.

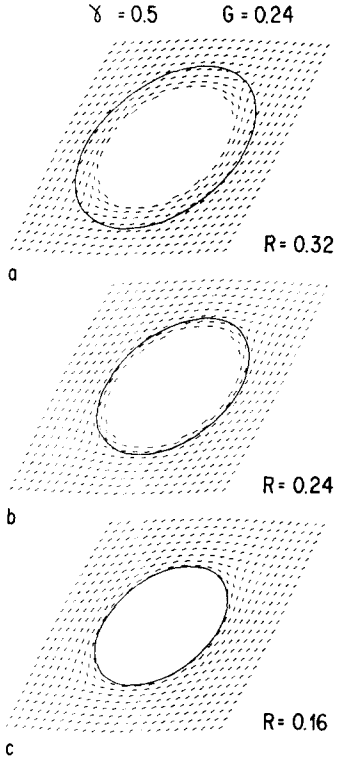

Fig. 9. Flattening plane trajectories and position of triple points relative to the pluton boundary for circular ballooning. γ is the simple shear value, R is the ratio of initial radius of plutons over the model width, and G the ratio of radius increase over model width.

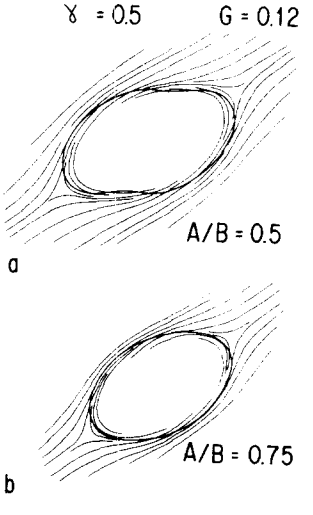

Fig. 10. Flattening plane trajectories and position of triple points for elliptical ballooning. A and B are the radius increases along Y and X. γ is the simple shear value and G the ratio of radius increase over model width.

At the extremities of the pluton, in the flattening domain, a local anomalous increase in K value may be seen (Figs. 11a and 12a). As the deformation increases, a constriction type strain may appear at the centre of the anomaly (Fig. 12b). These anomalies also contain triple points but not at their centre. This clearly shows that triple points are not the equivalent of finite neutral points in folds (Ramsay 1967, p. 147, Dieterich 1969, Roberts & Strömgard 1972). The triple points of the present models correspond to narrow zones of constrictive strain, not to zones of no strain at all.

Variations in finite strain intensity

Let us take the small axis λ_3 of the strain ellipsoid as a measure of strain intensity. By comparison with the nominal value of λ_3 for simple shear only, maps of λ_3 values show that areas on the long sides of pluton are characterized by an increase in the amount of shortening and areas situated at the extremities by a decrease in the shortening (Figs. 11c & d and 12). The anomalously low λ_3 values are situated near triple points but not superimposed on them (Figs. 11c & d and 12b).

λ_1 attitude

The long axis λ_1 of the strain ellipsoid is horizontal almost everywhere. Only in a small zone situated on the inner side of the triple points, with respect to the pluton, is the λ_1 axis vertical (Figs. 11e & f and 12c).

DISCUSSION

The model above is purely kinematic and considers only two-dimensional displacements. To be more realistic such a model should consider mechanical effects, such as those due to temperature-dependent viscosity gradients around plutons, and take into account the necessarily three-dimensional nature of displacements. However, this simple model allows us to explain certain features observed in the field, such as foliation trajectory patterns.

First of all, the model supports the interpretation given above, that foliation triple points, are a consequence of interference between a local ballooning strain field and a regional strain field (Ledru & Brun 1977, Brun & Pons 1979). The model also explains how ballooning can control the position of triple points. Plutons from the Burguillos anticline give good examples of internal and external locations of foliation triple points (Fig. 3).

Secondly, the similarity between flattening plane trajectories in the case of elliptical ballooning (Fig. 10a) and foliation trajectories in Pattern B (Fig. 6) is interesting. It does suggest that ballooning in the case of the Salvatierra pluton is elliptical. In fact, this explanation is quite possible for the Salvatierra pluton which was the last to be

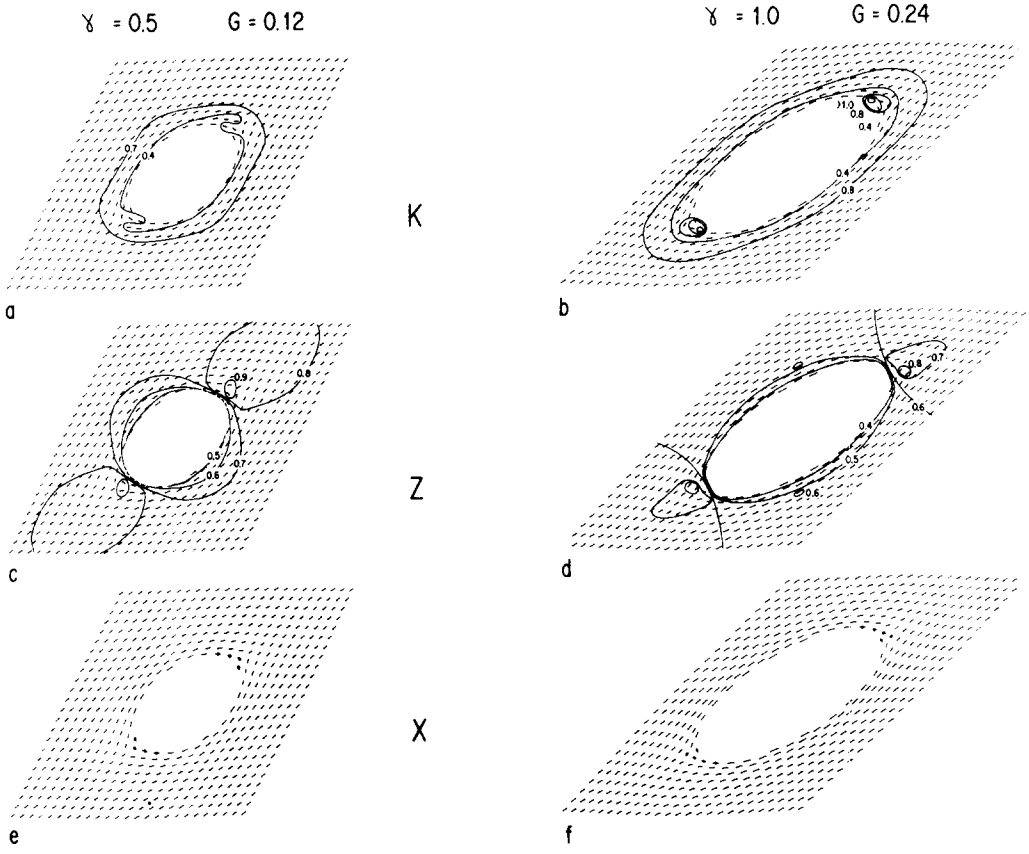

Fig. 11. Finite strain state for increasing values of γ and G for circular ballooning. (a) and (b) maps of K parameter ($K = (\lambda_1/\lambda_2 - 1)/(\lambda_2/\lambda_3 - 1)$, with $\lambda_1 > \lambda_2 > \lambda_3$, Flinn 1962). (c) and (d) maps of shortening (numbers refer to λ_3 or Z strain ellipsoid axis length). (e) and (f) position of λ_1 or X strain ellipsoid axis. Lines are horizontal X axes and dots vertical X axes.

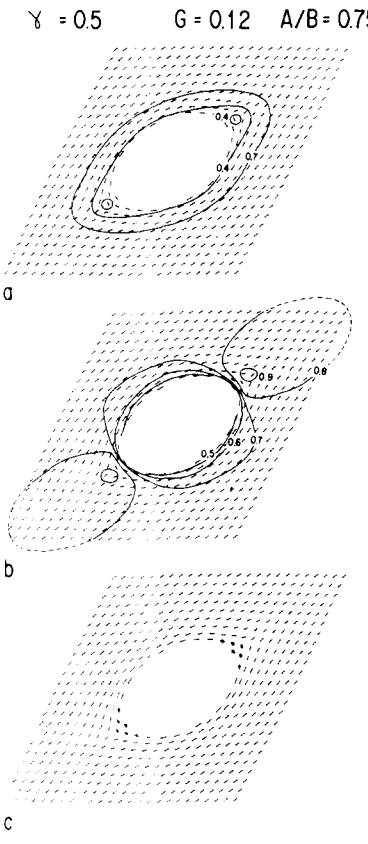

Fig. 12. Finite strain state for elliptical ballooning. (a) map of K parameter, (b) map of shortening and (c) position of X trains ellipsoid axis.

emplaced of the four plutons studied. At this time, the anticline was almost fully developed and the pluton could have inflated more easily along the anticlinal axis than perpendicular of it.

Variations in the finite strain ellipsoid and in strain intensity have not been measured around the plutons within the Burguillos anticline but strain indications given by the models could be useful in further work.

Acknowledgements—Field work supported by the "Action Thematique Programmée: Tectonophysique" No. 4061 CNRS France. Computing facilities have been provided by the CNRS. We are grateful to P. Choukroune, P. R. Cobbold and C. Le Corre for helpful discussions and suggestions during the research. Thanks are also due to A. J. Barber, W. M. Schwerdtner, P. R. Cobbold, and an anonymous referee for many improvements and careful checking of the manuscript, and to A. Le Moigne and M. Lautram for typing and drafting.

REFERENCES

Bard, J. P. 1965. Introduction à la géologie de la chaîne hercynienne dans la Sierra Morena occidentale (Espagne). Hypothèses sur les caractères de l'évolution géotectonique de cette chaîne. *Revue Géogr. phys. Géol. dyn.* **7**, 323–337.

Bard, J. P. 1969. Le métamorphisme régional progressif des Sierras d'Aracena en Andalousie occidentale (Espagne). Sa place dans le segment hercynien sub-ibérique. Thés. Fac. Sci. Univ. Montpellier.

Berger, A. R. & Pitcher, W. S. 1970. Structures in granitic rocks: a commentary and a critique on granite tectonics. *Proc. Geol. Ass.* **81**, 441–461.

Berthé, D., Choukroune, P. & Jégouzo, P. 1979. Orthogneiss, mylonite and non coaxial deformation of granites: the example of the South Armorican Shear Zone. *J. Struct. Geol.* **1**, 31–42.

Bladier, Y. & Laurent, P. 1974. Etude d'un décrochement profond synmétamorphique: le 'couloir' blastomylonitique de Badajoz–Cordoba. *2ème Réun. A. Sci. Terre, Pont-à-Mousson (Nancy)*, 52.

Brun, J. P. & Pons, J. 1979. Existe-t-il des granites post-tectoniques dans la chaîne hercynienne ? *Réun. Ann. Sci. Terre. Lyon.*

Brun, J. P. & Pons, J. 1981. Patterns of interference between granite diapirism and regional deformation (abstract). In: Coward, M. P. Diapirism and Gravity Tectonics: Report of a Tectonic Studies Group conference held at Leeds University, 25–26 March 1980. *J. Struct. Geol.* **3**, 93.

Burg, J. P., Iglesias, M., Laurent, Ph., Matte, Ph. & Ribeiro, A. 1980. Variscan intracontinental deformation, the Coimbra-Cordoba shear zone (SW Iberian Peninsula). *Int. Conf. "The Effect of Deformation on Rocks"*, Gottingen, abstracts, 51–54.

Clifford, P. M., 1972. Behavior of an Archean granitic batholith. *Can. J. Earth Sci.* **9**, 71–77.

Dieterich, J. H. Origin of cleavage in folded rocks. *Am. J. Sci.* **267**, 155–165.

Dupont, R., Linares, E. & Pons, J. in press. Premières datations radiométriques par la méthode Potassium–Argon des granitoïdes de la Sierra Morena occidentale (Province de Badajoz, Espagne): Conséquences géologiques et métallogéniques. *Bol. Geol. Min. Inst. Geol. Min. Espana.*

Efimov, N. V. 1966. *An Elementary Course in Analytical Geometry*. Part 2. Pergamon, London, pp. 150.

Flinn, D. 1962. On folding during three-dimensional progressive deformation. *Q. Jl geol. Soc. Lond.* **118**, 385–433.

Fyfe, W. S. 1973. The generation of batholiths. *Tectonophysics* **17**, 273–283.

Grout, F. F. 1945. Scale models of structures related to batholiths. *Am. J. Sci.* **243A**, 260.

Holder, M. T. 1979. An emplacement mechanism for post-tectonic granites and its implications for their geochemical features. In: *Origin of Granite Batholiths–Geochemical Evidence.* (edited by Atherton M. P. & Tarney, J.) Shiva Publishing Limited, Orpington U.K., 116–128.

Holder, M. T. 1981. Some aspects of intrusion by ballooning: the Ardara pluton (abstract). In: Coward, M. P. Diapirism and Gravity Tectonics: report of a Tectonic Studies Group conference held at Leeds University, 25–26 March 1980. *J. Struct. Geol.* **3**, 93.

Jaeger, J. C. 1969. *Elasticity, Fracture and Flow.* Methuen, London.

Jaeger, J. C. & Cook, N. G. W. 1971. *Fundamentals of Rock Mechanics.* Chapman & Hall, London.

Ledru, P. & Brun, J. P. 1977. Utilisation des fronts et des trajectoires de schistosité dans l'étude des relations entre tectonique et intrusion granitique: exemple du granite de Flamanville (Manche). *C. r. hebd. Séanc. Acad. Sci., Paris* **258**, 1199–1202.

Morgan, J. 1980. Deformation due to the distension of cylindrical igneous contacts: a kinematic model. In: *Analytical Studies in Structural Geology.* (edited by Schwerdtner, W. M., Hudleston, P. J. & Dixon, J. M.). *Tectonophysics* **66**, 167–178.

Pitcher, W. S. 1979. The nature, ascent and emplacement of granitic magmas. *J. geol. Soc. Lond.* **136**, 627–662.

Pons, J. 1975. Pétrofabrique des roches éruptives dans les complexes de Querigut (Ariège, France) et de Burguillos del Cerro (Badajoz, Espagne). *Pétrologie* **1**, 209–223.

Ramberg, H. 1967. *Gravity, Deformation and the Earth's Crust.* Academic Press, London.

Ramberg, H. 1970. Model studies on relation to intrusion of plutonic bodies. In: *Mechanism of Igneous Intrusion* (edited by Newall, G. & Rast, N.) *Geol. J.* Spec. Issue **2**, 261–285.

Ramberg, H. 1975. Superposition of homogeneous strain and progressive deformation in rocks. *Bull. geol. Inst. Univ. Uppsala*, **6**, 35–67.

Ramsay, J. G. 1962. Interference patterns produced by the superposition of folds of similar type. *J. Geol.* **70**, 466–481.

Ramsay, J. G. 1967. *Folding and Fracturing of Rocks.* New York, McGraw Hill.

Ramsay, J. G. 1981. Emplacement mechanics of the Chindamora batholith, Zimbabwe (abstract). In: Coward, M. P. Diapirism and Gravity Tectonics: report of a Tectonic Studies Group conference at Leeds University, 25–26 March 1980. *J. Struct. Geol.* **3**, 93.

Roberts, D. & Strömgard, K. E. 1972. A comparison of natural and experimental strain patterns around fold hinges. *Tectonophysics* **14**, 105–120.

Schwerdtner, W. M. 1972. Behaviour of an archean granitic batholith: discussion. *Can. J. Earth Sci.* **9**, 1230–1234.

Vauchez, A. 1975. Tectoniques tangentielles superposées dans le segment hercynien sud-ibérique: les nappes et plis couchés de la région d'Alconchel-Fregenal de la Sierra (Badajoz). *Bol. Geol. Min. Inst. Geol. Min. Espana* **86,** 573–580.

Whitehead, J. A. Jr & Luther, D. S. 1975. Dynamics of laboratory diapir and plume models. *J. geophys. Res.* **80,** 705–717.

APPENDIX

Procedure for computation of the model

Computations have been made on a small digital computer (Hewlett Packard 9821). The principal strain maps (Figs. 9, 10, 11 and 12) have been obtained directly from an automatic plotter on line. Contours of K, Z (Figs. 10 and 11) and flattening plane trajectories (Fig. 12) have been smoothed by hand.

Finite strain. From the initial (X, Y) and final (X'', Y'') coordinates, the deformation gradients a, b, c and (Fig. 13) are determined following the convention used by Ramsay (1967, p. 57). a and d represent extension along the X and Y axes; b and c represent shears. That is,

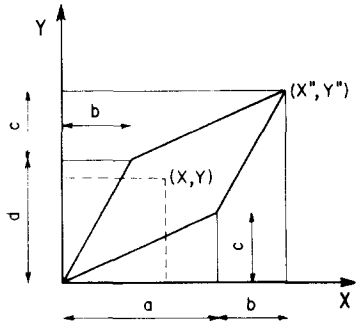

Fig. 13. Determination of principal strains.

$$X'' = aX + bY,$$

$$Y'' = cX + dY,$$

or

$$X = \frac{dx'' - by''}{ad - bc}, \tag{6a}$$

$$Y = \frac{-cX'' + ay''}{ad - bc}. \tag{6b}$$

Taking the equation of a circle,

$$X^2 + Y^2 = 1, \tag{7}$$

and substituting (6) in (7), we obtain:

$$(c^2 + d^2)\,X''^2 - 2(ac + bd)\,X''Y'' + (a^2 + b^2)\,Y''^2 = (ad - bc)^2, \tag{8}$$

which represents the strain ellipse (cf. Jaeger 1969, p. 26–27).

Written in matrix form (Efimov 1966, Ramberg 1975), (8) becomes:

$$(X'', Y'') \cdot \begin{bmatrix} \frac{c^2+d^2}{\Delta} & -\frac{(ac+bd)}{\Delta} \\ + & \\ -\frac{(ac+bd)}{\Delta} & \frac{a^2+b^2}{\Delta} \end{bmatrix} \begin{bmatrix} X'' \\ \cdot \\ Y'' \end{bmatrix} = 1, \tag{9}$$

where $\Delta = (ad - bc)^2$.

The principal axes ($\lambda_1 > \lambda_2$) of the finite strain ellipse can be obtained directly from the eigenvalues E1 and E2 of the square matrix in (9), that is:

$$\lambda_1 = 1/\sqrt{(E_1)}; \quad \lambda_2 = 1/\sqrt{(E_2)}.$$

The orientations of principal strain axes are the orientations of the corresponding eigenvectors of the square matrix in (9).

The third axis λ_3 is obtained assuming no volume change:

$$\lambda_1 \times \lambda_2 \times \lambda_3 = 1.$$